RSC Advances



This is an *Accepted Manuscript*, which has been through the Royal Society of Chemistry peer review process and has been accepted for publication.

Accepted Manuscripts are published online shortly after acceptance, before technical editing, formatting and proof reading. Using this free service, authors can make their results available to the community, in citable form, before we publish the edited article. This Accepted Manuscript will be replaced by the edited, formatted and paginated article as soon as this is available.

You can find more information about *Accepted Manuscripts* in the **Information for Authors**.

Please note that technical editing may introduce minor changes to the text and/or graphics, which may alter content. The journal's standard <u>Terms & Conditions</u> and the <u>Ethical guidelines</u> still apply. In no event shall the Royal Society of Chemistry be held responsible for any errors or omissions in this *Accepted Manuscript* or any consequences arising from the use of any information it contains.



Glycine-assisted synthesis of NiO hollow cage-like nanostructures for sensitive nonenzymatic glucose sensing

Zafar Hussain Ibupoto^a, Aynam Nafady^{b,c}, Razium Ali Soomro^{d, *}, Sirajuddin^d, Syed Tufail Hussain Sherazi^d, Muhammad Ishaq Abro^e, Magnus Willander^f

^a Dr M.A Kazi Institute of chemistry university of Sindh Jamshoro, 76080, Pakistan
 ^b Department of Chemistry, Sohag University, Cairo, 8252, Egypt
 ^c Department of Chemistry, College of Science, King Saud University, Riyadh 11451, Saudi Arabia
 ^d National Center of Excellence in Analytical Chemistry, University of Sindh, Jamshoro, 76080, Pakistan

^e Department of Metallurgy and Materials Engineering, Mehran University of Engineering & Technology, Jamshoro 76080, Pakistan

^fDepartment of Science and Technology, Campus Norrkoping, Linkoping University, SE-60174 Norrkoping, Sweden

Abstract

In this work, a highly sensitive non-enzymatic glucose sensor was developed based on NiO hollow cage-like nanostructures (NiO HCs). The novel structures were synthesized using hydrothermal growth route with glycine employed as a growth director. The as-synthesized NiO HCs were characterized by using scanning electron microscopy (SEM), X-ray photoelectron microscopy (XPS) X-ray diffraction (XRD) and Fourier transform infrared (FTIR) techniques for morphological, compositional and structural determination respectively. The prepared NiO HCs were directly integrated to be structured electrodes exhibiting enhanced electrocatalytic performance toward the oxidation of glucose with high sensitivity (2476.4 µA mM⁻¹cm⁻²), Low detection limit (LOD) (0.1 µM), wide detection range (0.1-5.0 mM) (r²=0.99) and excellent reproducibility. The developed non-enzymatic glucose sensor further demonstrated excellent anti-interference property in the presence of common interferents' such as uric acid (UA), dopamine (DP) and ascorbic acid (AS). The role of glycine molecules was as a growth directing agent and a plausible mechanism has also been highlighted. In addition, the NiO HCs modified electrode was also used to analyze glucose concentration in human serum samples. The excellent sensing performance can be attributed to the unique morphology, which allowed increased electron transfer passages with lower charge transfer resistance, and enhanced molecular approach during electrochemical sensing offered from nanoscale "hollow cage" units of NiO structures.

Keywords: Glycine, NiO nanostructures, enzyme free glucose sensor, cyclic voltammetry

*Corresponding author. Tel.: + 92 336 3051253; Fax: + 92 22 9213431

E-mail address: raziumsoomro@gmail.com (Razium Ali Soomro)

1. Introduction

The electrical properties of various metal oxides have wide range of spectrum including from conductors to semiconductors and insulators ¹. In the recent past, nanoscale semiconducting metal oxides have been actively and potentially used in the different fields because of their attractive and unique electronic, mechanical and optical properties. The bulk semiconducting metal oxides, their properties have been strongly investigated and collected, however compare to bulk phase of metal oxides, the nanoscale metal oxides have low dimensions, high surface to volume ratio, high crystalline quality, and a Debye length (D) relative to its sizes ². These highlighted properties of nanoscale semiconducting metal oxides make them a strong and potential candidate for the fabrication of nanodevices such as efficient catalyst, and in the development of sensitive sensors. Different growth techniques including vapour phase transport ³, electrospinning ^{4, 5}, laser ablation ⁶, arc discharge ⁷, template assisted methods⁸, and low temperature aqueous chemical growth technique ⁹ have previously been adapted and used for the synthesis of different nanoscale metal oxides. However, hydrothermal method is well known and most commodiously used because of its advantages like low temperature, economic feasibility, environment friendliness, and simplicity.

At the present, the determination of glucose concentration is an important task to be performed in biotechnology, clinical diagnostics, and food industry. Hence, there is an increasing need of portable, sensitive and selective glucose sensors for the routine determination of glucose. The glucose detection is performed by two methods i.e. one involving glucose oxidase and other method is enzyme free. The conventional glucose biosensors are fabricated by using glucose oxidase which favours the selective oxidation of glucose in the presence of O₂ to produce hydrogen peroxide ¹⁰⁻¹². Although the sensitive, glucose oxidase based biosensors are associated with certain issues like complexity in the immobilization of enzyme, denaturation of the enzyme and expensive, restricting its wide acceptance in various applications. To overcome these limitations of enzyme based glucose biosensors, much attention is paid in the recent time for the development of enzyme free glucose sensors ¹³. In the fabrication and design of several non-enzymatic glucose sensors different materials are used such as precious metals Pt, Au, Ag and alloy-metals ^{14, 15}. It has been reported that several metal oxides have been used in the fabrication of enzyme free glucose sensors such as NiO, CuO, MnO₂, and Co₃O₄ ¹⁶⁻¹⁸. Recently, NiO nanostructures have also been potentially used in the fabrication of enzyme free glucose sensors including nanofibers ^{19, 20}, nanoparticles ^{21, 22}, nanoflakes ²³, and hollow spheres ²⁴. The use of template during the growth of metal oxides for the control of dimension and morphology is an attractive route to obtain the reproducible nanomaterial of high interest. Particularly, biotemplates like amino acids and proteins are getting much attention due to their green nature and efficiency in the formation for unique structures with controlled morphology, which exhibits enhanced electrochemical properties contrary to the conventional nanostructures.

In the present study glycine amino acid for the first time has been explored for its potential in the directing growth of NiO nanostructure. The as-synthesized NiO HCs were further employed for development of highly sensitive, selective and robust non-enzymatic glucose sensor. The presented glucose sensor was further applied in the analysis of glucose from real blood serum and obtained results were in full agreement with those obtained with commercially available glucometer.

2. Experimental

2.1. Materials

Analytical grade nickel nitrate hexahydrate (Ni(NO₃)₂.6H₂O), glycine (C₂H₅NO₂), 33 % ammonia (NH₃), D-glucose (C₆H₁₂O₆), dopamine (C₈H₁₁NO₂), ascorbic acid (C₆H₈O₆), uric acid (C₅H₄N₄O₃) and sodium hydroxide (NaOH) were purchased from Sigma Aldrich. 1.0 % nafion was prepared in isopropanol (Merck),

2.2. The glycine assisted synthesis of NiO HCs

The hydrothermal method was used for the synthesis of hollow cages of NiO nanostructures using glycine as bio template. A 0.1M (Ni(NO₃)₂.6H₂O) solution was prepared in 100 mL of deionized water and 5 mL of 33% (NH₃) was also added in the solution, followed by 1.0 gram of (C₂H₅NO₂). After complete homogenization, the growth solution was kept in the preheated electric oven at 95°C for 4-6 hours. Glycine-aided Ni(OH)₂ nanostructures were collected and washed to remove residual impurities after the completion of growth process. The obtained material was further annealed at 450°C for 2-3 hours in order to acquire pure phase NiO hollow cage-like nanostructures.

2.3. The characterization and electrochemical measurement of NiO nanostructures

Scanning electron microscopy (SEM) (Jeol, Japan) was employed for morphological studies; X-ray diffraction (XRD) (D-8 of Bruker) contributed towards phase determination of obtained material; X-ray photoelectron microscopy (XPS) determined chemical composition and Fourier transform infrared spectroscopy (FTIR) (Nicolet 5700 of Thermo) was used for chemical bonding studies. The entire electrochemical experiments were accomplished using Bipotentiostate model 760 USA.

2.4. The modification of glassy carbon electrode with hollow cage-like NiO nanostructures

Prior to the surface modification, glassy carbon electrode (GCE, diameter 3 mm) was polished with 1 μ m and 0.05 μ m alumina paste respectively, and then the cleaned with deionized water. Then electrode was further sonicated in ethanol and di-ionized water to remove any external impurities and consequently dried at room temperature.

The polished bare glassy carbon electrode was modified (NiO HCs-Nafion/GCE) via drop casting 5 μ L of ethanol dispersed hollow cage-like NiO nanostructures (5 mg/ml). Complete adhesion of NiO over electrode was ensured by depositing 5 μ L drops of 1% nafion solution.

The finally obtained NiO HCs-Nafion/GCE was used as working electrode during the entire glucose sensing experiments.

2.5 Electroanalysis

Electroanalysis was carried using cyclic voltammetry (CV) as a primary mode for measurements. The electrochemical cell system was based on three electrode system. Silver-silver chloride (silver-silver chloride wire (Ag/AgCl)) was used as a reference electrode; platinum (platinum (Pt)) electrode was used as a counter electrode and NiO HCs-Nafion/GCE was used as a working electrode. All the experiments for the enzyme free sensing of glucose were performed in 0.1 M electrolytic solution of NaOH with initial potential range, 0 to 0.7 (V), scan rate, 0.05 (V/s), quiet time, 5 (sec), and sensitivity, 1×10^{-6} (A/V).

2.6 The determination of glucose from human blood serum

Blood glucose concentration was estimated using NiO HCs-Nafion/GCE. The human blood was obtained from few individuals and properly treated to obtain the samples suitable for the electrochemical analysis. The blood sera were separated using high speed centrifugation (25 min) followed by proper dilution with 0.1M NaOH. Analysis was done in similar fashion as mentioned in section 2.5 and results were confirmed and validated by correlating them with those obtained by a commercial glucometer.

3. Results and discussion

3.1. The characterization of hollow cage-like NiO nanostructures

The novel nanostructures of NiO were synthesized via hydrothermal growth method. Fig.1 represents the XRD pattern obtained for hollow cage-like NiO with three prominent and sharp diffraction peaks at 20 of 43.16, 62.77, and 75.30.The peaks are indexed to face-centered cubic (FCC) structure of NiO belonging to (200), (220), and (311) crystal planes as depicted by standard Joint Committee on Powder Diffraction Standards (JCPDS No. 71-1179) ^{25, 26}. The data obtained clearly suggest the formation of purely crystalline NiO material.

Fig.1

The morphological features of synthesized materials were highlighted by SEM. Fig. 2 shows the low and high resolution SEM images of NiO respectively. Fig. 2(a, b) reveal that NiO nanomaterial exhibits a hollow cage-like morphology. Fig.2 (b, c) presents high resolution images reflecting tapering features of individual cage. It can be seen that the formation of such structures is via interconnected small nano pellets, which further aggregates to give a spherical hollow-cage shaped structure with an average dimension of 100 to 200 nm.

Fig. 2

Further chemical composition assessment was carried using XPS analysis of hollow-cage shaped NiO nanostructures. The wide scan spectrum provided in Fig. 3(a) only contains Ni and O peaks indication highest compositional purity of synthesized product. The Fig. 3(b)

Page 5 of 23

obtained for Ni 2p shows the presence of corresponding Ni $2p^{1/2}$ and Ni $2p^{3/2}$ peaks located at 873.0 and 885.9 eV with spin orbit splitting gap of 12.9 eV. Similarly the major peak of O 1s shown in Fig. 3(c) resides at 529.8 eV. The obtained peak positions are in full agreement with pure NiO 27,28 .

Fig. 3

FTIR spectra were recorded both before and after calcination of NiO for better insight of growth mechanism. Fig.4(a) represents the FTIR spectra of glycine assisted precursor (Ni(OH)₂) with important glycine -NH₂ stretching at 3341 and -C=O at 1783 cm⁻¹, while other bands can be attributed to different structural units associated with glycine molecules^{29, 30}. When comparing the both FTIR spectra a slight shift in frequencies of -NH₂ and -C=O from 3341 and 1783 to 3325 and 1805 cm⁻¹ is observed respectively. Such shifts in vibrational frequencies Cleary depicts the interlinkage between metal oxide and amino acid is via -NH₂ and -C=O groups of glycine. The presence of band near 500 cm⁻¹ in Fig 4(b) is attributed to metal-oxide stretching vibration.

Fig. 4

The FTIR clearly suggests that the NiO growth is assisted via amino group and carboxyl group which as reported previously possesses selective absorptivity and special metal cation complexation properties and can serve as an effective growth directing agent⁴.

Thus, using SEM, XPS, and FTIR information a plausible growth mechanism is suggested in scheme.1

Scheme.1

Based on the classical anisotropic growth direction, at the initial stage Ni (OH) 2 nuclei are directed to form nanoplates. Glycine however, owning to its capability of selective absorption and special metal cation complexation properties ³¹ easily adsorbs onto the surface of newly formed nuclei leading to spontaneous aggregation. These aggregated nuclei further grow spherical in shape with void spaces enclosed within. In addition, since there are strong hydrophobic interactions between glycine molecules, initial growth of nuclei is associated with branch formation which as a consequence allows formation of hollow-cage, shaped NiO nanostructures.

3.2 The enzyme free detection of glucose using glycine directed novel hollow cage-like NiO nanostructures

To explore the electrocatalytic properties of novel nanostructures of NiO, the electrocatalytic properties of novel NiO nanostructures were evaluated using NiO HCs-Nafion/GCE for the enzyme free oxidation of glucose. The electrochemical assessment of glucose was done using CV as a primary technique.

CV profile for both bare and modified electrodes were recorded in the absence and presence of 1mM glucose and are presented in Fig. 5. It can be clearly seen that no significant response can be recorded for bare glassy carbon both in absence and presence of glucose molecules. In contrast, NiO HCs-Nafion/GCE in presence of 1.0 mM glucose showed prominent oxidation peak with increased current response (Ip) which could be assigned to Ni(II)/(III) ²⁴. Such phenomenon of an excellent electrochemical response could be attributed to the porous nature

and high surface area possessed by as prepared novel nanostructures of NiO. The behaviour of presented NiO modified electrode is according to the existing glucose sensors composed of NiO nanostructures $^{19-21, 32, 33}$. Although the direct electro catalytic oxidation of glucose at nickel oxide hollow structures is unclear till today, but based on various literature reports Ni(II)/(III) redox couples is considered to be responsible for direct oxidization of glucose. At the initial stage where glucose molecules adsorbs over the surface of NiO hollow cages, Ni²⁺ as a consequence of applied potential, electro-oxidize within the alkaline medium to produce Ni³⁺ as represented by equation (1). This result in the release of electrons which concurrently are responsible for generation of large anodic peak current and oxidation of glucose to gluconic acid ($C_6H_{12}O_7$) by Ni³⁺ which at the same time gets de-oxidized to Ni²⁺ as shown in equation (2). This system cycles continuously and with an increase in concentration of glucose, the anodic peak current is simultaneously observed to increase $^{23, 34, 35}$.

The NiO HCs-Nation/GCE electrode with hollow cage shaped morphologies allows enhanced electron transfer from the electrode to the surface residing glucose molecules based on their large surface area. In addition, the high density of developed NiO hollow cages with large spacing among the cage like units not only would provide greater number of Ni(II)/Ni(III) redox couples but also facilitate the faster diffusion of glucose molecules. Thus, it is safe to that enhance electrical properties can be obtained by synthesizing NiO with hollow cage shaped morphological features. Fig. S1 provides a schematic diagram of the working electrode with a simplified mechanism for enzyme free glucose sensing using NiO hollow cage modified glassy carbon electrode (GCE).

Fig. 5

To ensure best and reproducible quality of the developed sensor, the optimization of most important parameters for peak current improvement were done in 1.0 mM glucose using NiO HCs-Nafion/GCE. The study of catalytic kinetic of glucose oxidation and reduction peak using novel nanostructures of NiO was performed by evaluating the effect of scan rate on the current response. The observed and recorded cyclic voltammetry response for the scan rate is shown in Fig 6(a). The inset shows the linear response of NiO HCs-Nafion/GCE with square root of scan rate in range from 0.05-1.0 V/s. This study explored that the response of NiO modified electrode for the redox process is diffusion controlled.

The effect of nanostructured deposition volume over peak current (Ip) was also investigated and corresponding CV profile is shown in Fig. 6(b). Different volumes including 5, 10, and 15 μ L were selected for electrode modification similarly as mentioned in previous section (2.4). An increased Ip response was recorded with successive increment in nanostructure casting volume. However, 5 μ L was selected as optimum volume based on its stable and reproducible response. At much higher volumes (> 5 μ L) decrease in Ip was noted which may be attributed to erosion of nanomaterial from surface of electrode. In addition to this, the effect of electrolytic (NaOH) volume on the electrochemical response of the modified

electrode was also investigated as depicted in Fig. 6(c). Ip response was recorder in range from 1-10 ml of electrolytic volume. A shift in the oxidation peak to lower potential with increase in pH can be clearly seen, however maximum Ip response was obtained at 9 ml of electrolytic suggesting optimum performance of electrode.

Fig. 6

The important analytical data was obtained by plotting a linear calibration graph between Ip response (0.48 V) of NiO HCs-Nafion/GCE and glucose concentration in range between 0.1 to 5.0 mM as presented in Fig. 7(a). Linear regression analysis (Fig.7 (b)) evaluated excellent linearity with correlation of determination (r^2) as 0.9997. The developed sensor demonstrated excellent sensitivity of 2476.4 μ A mM⁻¹ cm⁻² which was calculated by dividing the obtained slope (173.35 μ A mM⁻¹) from calibration with the standard area of GCE (0.07 cm⁻²). The LOD and limit of quantification (LOQ) calculated as 0.1 (S/N = 3) and 3.3 μ M respectively. The effective area of NiO HCs-Nafion/GCE was estimated by comparing its current density with that obtained by GCE modified by planer NiO surface. The planer NiO material was synthesized via similar procedure presented in section (2.2), but in the absence of glycine biotemplate which inhabited the formation of hollow cage like morphology. The corresponded CV profile is presented in Fig. S2 where, the calculated effective area of 0.30 cm⁻² was obtained by the following formula:

$$\frac{Q_{\text{NiO HCs-MGCE}}}{Q_{\text{NiO (Planer) GCE}}} = \frac{A_{\text{NiO HCs-MGCE}}}{A_{\text{GCE}}}$$

The estimated effective electrode area is about 4.28 times higher than that of standard GCE.

Fig.7

The electrochemical performance of the developed sensor was compared with other non-enzymatic glucose sensor systems. The data is provided in Table 1 and it can be seen that the presently developed sensor offer greater sensitivity with lower LOD values and wider detection window making it far more superior to the mentioned sensors.

3.3 Selectivity, reproducibility and stability of developed sensor

Selectivity is a crucial parameter in evaluating performance of the non-enzymatic glucose sensors in the presence of common interferents. For glucose sensing, uric acid (UA); dopamine (DP) and ascorbic acid (AA) are considered most common interferents ³⁶. Thus, CV response was recorded for 0.1 mM UA, DP and AA in addition to 1.0 mM glucose using NiO HCs-Nafion/GCE as shown in Fig. 8(a). No considerable change in response of NiO HCs-Nafion/GCE was noted which suggested excellent selectivity of the developed sensor. The reproducibility of developed sensor was measured by modifying 15 bare glassy carbon electrodes with similar methodology as described section (2.4). These modified electrodes were further used for anodic peak current measured in 1.0 mM glucose solution. The data obtained reveled < 1.0 % relative standard deviation (RSD) for anodic peak current (Fig.8 (b)) suggesting high reproducibility of developed sensor. The assessment of stability for the developed sensor was done by measuring NiO HCs-Nafion/GCE response in 1.0 mM glucose

solution up to 2 months. The obtained SV profile (Fig. 8(c)) suggests retention of more than 95% of initial current, indicating extreme stability of present sensor.

Fig. 8

3.2. The non-enzymatic glucose sensing of real samples

The modified NiO HCs-Nafion/GCE was successfully used for the estimation of glucose from human blood. The blood samples were obtained from known personals and the corresponding blood sera were separated by high speed centrifuge. The prepared samples were further properly diluted and classified in random and fasting sugar categories. The blood glucose was estimated using linear equation mentioned in section (3.2) and was determined in range between 4.8 to 5.9 mM and 4.5 to 4.9 mM for random and fasting sugar respectively.

Validation of obtained results was done by comparing the measured concentrations with those obtained by commercial glucometer. Table 2 presents the obtained glucose concentrations for each sample. The study clearly demonstrates the potential of developed sensor in the routine estimation of glucose level.

4. Conclusion

In this research study, glycine assisted novel hollow cage-like NiO nanostructures were prepared by hydrothermal growth method. The synthesized nanostructures possessed excellent porosity which favours its application in the development of sensitive and selective enzyme free glucose sensor. The study also presents the growth mechanism of hollow cage-like NiO nanostructures signifying the role of glycine molecules as growth directing agent. The developed sensor exhibits excellent sensitivity, high stability and wider working spectrum compared to other NiO based non-enzymatic glucose sensors. Further more the developed sensor has shown potential and reliable response in the monitoring of glucose from real blood samples proving its feasibility for the routine estimation of glucose level in real human blood sample analysis.

Acknowledgments

We acknowledge the Higher Education Commission, Islamabad, Pakistan for provision of financial assistance during this research and National centre of excellence in analytical chemistry Jamshoro for their facilities. The authors equally highly thank and cordially appreciate the financial support by King Saud University via their Research Project No. RGP-VPP-236.

References

- 1. E. Comini, *Anal Chim Acta*, 2006, 568, 28-40.
- 2. A. Kolmakov and M. Moskovits, Annual Review of Materials Research, 2004, 34, 151-180.
- 3. M. H. Huang, Y. Wu, H. Feick, N. Tran, E. Weber and P. Yang, *Advanced Materials*, 2001, 13, 113-116.
- 4. H. Y. Zhu, Y. Lan, X. P. Gao, S. P. Ringer, Z. F. Zheng, D. Y. Song and J. C. Zhao, *Journal of the American Chemical Society*, 2005, 127, 6730-6736.
- 5. N. A. M. Barakat, M. S. Khil, F. A. Sheikh and H. Y. Kim, *J. Phys. Chem C*, 2008, 112, 12225-12233.
- 6. Z. Liu, D. Zhang, S. Han, C. Li, T. Tang, W. Jin, X. Liu, B. Lei and C. Zhou, *Advanced Materials*, 2003, 15, 1754-1757.
- 7. Y. C. Choi, W. S. Kim, Y. S. Park, S. M. Lee, D. J. Bae, Y. H. Lee, G. S. Park, W. B. Choi, N. S. Lee and J. M. Kim, *Advanced Materials*, 2000, 12, 746-750.
- 8. J. C. Hulteen and C. R. Martin, *J. Mater. Chem*, 1997, 7, 1075-1087.
- 9. M. Yoshimura and S. Sōmiya, *Mater Chem Phys*, 1999, 61, 1-8.
- 10. S. Liu, J. Tian, L. Wang, Y. Luo, W. Lu and X. Sun, *Biosens Bioelectron*, 2011, 26, 4491-4496.
- 11. C. Shan, H. Yang, D. Han, Q. Zhang, A. Ivaska and L. Niu, *Biosens Bioelectron*, 2010, 25, 1070-1074.
- 12. B. Wu, G. Zhang, S. Shuang and M. M. Choi, *Talanta*, 2004, 64, 546-553.
- 13. A. Sun, J. Zheng and Q. Sheng, *Electrochim. Acta*, 2012, 65, 64-69.
- 14. Y. Li, Y.-Y. Song, C. Yang and X.-H. Xia, *Electrochem. Commun*, 2007, 9, 981-988.
- 15. Y. Y. Song, D. Zhang, W. Gao and X. H. Xia, *Chemistry*, 2005, 11, 2177-2182.
- 16. Y. Zhang, F. Xu, Y. Sun, Y. Shi, Z. Wen and Z. Li, *J. Mater. Chem*, 2011, 21, 16949-16954.
- 17. L.-C. Jiang and W.-D. Zhang, *Biosens. Bioelectron*, 2010, 25, 1402-1407.
- 18. Y. Ding, Y. Wang, L. Su, M. Bellagamba, H. Zhang and Y. Lei, *Biosens. Bioelectron*, 2010, 26, 542-548.
- 19. F. Cao, S. Guo, H. Ma, D. Shan, S. Yang and J. Gong, *Biosens. Bioelectron*, 2011, 26, 2756-2760.
- 20. Y. Ding, Y. Liu, L. Zhang, Y. Wang, M. Bellagamba, J. Parisi, C. M. Li and Y. Lei, *Electrochim. Acta*, 2011, 58, 209-214.
- 21. W.-D. Zhang, J. Chen, L.-C. Jiang, Y.-X. Yu and J.-Q. Zhang, *Microchim Acta*, 2010, 168, 259-265.
- 22. S. Kaneko, T. Ito, Y. Hirabayashi, T. Ozawa, T. Okuda, Y. Motoizumi, K. Hirai, Y. Naganuma, M. Soga, M. Yoshimoto and K. Suzuki, *Talanta*, 2011, 84, 579-582.
- 23. G. Wang, X. Lu, T. Zhai, Y. Ling, H. Wang, Y. Tong and Y. Li, *Nanoscale*, 2012, 4, 3123-3127.
- 24. C. Li, Y. Liu, L. Li, Z. Du, S. Xu, M. Zhang, X. Yin and T. Wang, *Talanta*, 2008, 77, 455-459.
- 25. S. Deki, H. Yanagimoto, S. Hiraoka, K. Akamatsu and K. Gotoh, *Chemistry of Materials*, 2003, 15, 4916-4922.
- 26. Y. Wang, Q. Zhu and H. Zhang, *Chem Commun*, 2005, DOI: 10.1039/B508807K, 5231-5233.
- 27. M. Chigane and M. Ishikawa, *Journal of the Chemical Society, Faraday Transactions*, 1998, 94, 3665-3670.
- 28. A. P. Grosvenor, M. C. Biesinger, R. S. C. Smart and N. S. McIntyre, *Surface Science*, 2006, 600, 1771-1779.
- 29. G. Fischer, X. Cao, N. Cox and M. Francis, *Chem. Phys.*, 2005, 313, 39-49.
- 30. R. Linder, K. Seefeld, A. Vavra and K. Kleinermanns, Chemical Physics Letters, 2008, 453, 1-6.
- 31. D. Xie, Q. Su, Z. Dong, J. Zhang and G. Du, CrystEngComm, 2013, 15, 8314-8319.
- 32. Y. Ding, Y. Liu, J. Parisi, L. Zhang and Y. Lei, *Biosens. Bioelectron*, 2011, 28, 393-398.
- 33. W. Lu, X. Qin, A. M. Asiri, A. O. Al-Youbi and X. Sun, *Anly*, 2013, 138, 429-433.
- 34. X. Li, A. Hu, J. Jiang, R. Ding, J. Liu and X. Huang, *J. Solid State Chem*, 2011, 184, 2738-2743.
- 35. R. M. Abdel Hameed, *Biosens. Bioelectron*, 2013, 47, 248-257.
- 1. E. Comini, Anal Chim Acta, 2006, **568**, 28-40.
- 2. A. Kolmakov and M. Moskovits, Annual Review of Materials Research, 2004, 34, 151-180.

- 3. M. H. Huang, Y. Wu, H. Feick, N. Tran, E. Weber and P. Yang, *Advanced Materials*, 2001, **13**, 113-116.
- 4. H. Y. Zhu, Y. Lan, X. P. Gao, S. P. Ringer, Z. F. Zheng, D. Y. Song and J. C. Zhao, *Journal of the American Chemical Society*, 2005, **127**, 6730-6736.
- 5. N. A. M. Barakat, M. S. Khil, F. A. Sheikh and H. Y. Kim, *The Journal of Physical Chemistry C*, 2008, **112**, 12225-12233.
- 6. Z. Liu, D. Zhang, S. Han, C. Li, T. Tang, W. Jin, X. Liu, B. Lei and C. Zhou, *Advanced Materials*, 2003, **15**, 1754-1757.
- 7. Y. C. Choi, W. S. Kim, Y. S. Park, S. M. Lee, D. J. Bae, Y. H. Lee, G. S. Park, W. B. Choi, N. S. Lee and J. M. Kim, *Advanced Materials*, 2000, **12**, 746-750.
- 8. J. C. Hulteen and C. R. Martin, *Journal of Materials Chemistry*, 1997, **7**, 1075-1087.
- 9. M. Yoshimura and S. Sōmiya, *Materials Chemistry and Physics*, 1999, **61**, 1-8.
- 10. S. Liu, J. Tian, L. Wang, Y. Luo, W. Lu and X. Sun, *Biosens Bioelectron*, 2011, **26**, 4491-4496.
- 11. C. Shan, H. Yang, D. Han, Q. Zhang, A. Ivaska and L. Niu, *Biosens Bioelectron*, 2010, **25**, 1070-1074
- 12. B. Wu, G. Zhang, S. Shuang and M. M. Choi, *Talanta*, 2004, **64**, 546-553.
- 13. A. Sun, J. Zheng and Q. Sheng, *Electrochimica Acta*, 2012, **65**, 64-69.
- 14. Y. Li, Y.-Y. Song, C. Yang and X.-H. Xia, Electrochemistry Communications, 2007, 9, 981-988.
- 15. Y. Y. Song, D. Zhang, W. Gao and X. H. Xia, *Chemistry*, 2005, **11**, 2177-2182.
- 16. Y. Zhang, F. Xu, Y. Sun, Y. Shi, Z. Wen and Z. Li, *Journal of Materials Chemistry*, 2011, **21**, 16949-16954.
- 17. L.-C. Jiang and W.-D. Zhang, Biosensors and Bioelectronics, 2010, 25, 1402-1407.
- 18. Y. Ding, Y. Wang, L. Su, M. Bellagamba, H. Zhang and Y. Lei, *Biosensors and Bioelectronics*, 2010, **26**, 542-548.
- 19. F. Cao, S. Guo, H. Ma, D. Shan, S. Yang and J. Gong, *Biosensors and Bioelectronics*, 2011, **26**, 2756-2760.
- 20. Y. Ding, Y. Liu, L. Zhang, Y. Wang, M. Bellagamba, J. Parisi, C. M. Li and Y. Lei, *Electrochimica Acta*, 2011, **58**, 209-214.
- 21. W.-D. Zhang, J. Chen, L.-C. Jiang, Y.-X. Yu and J.-Q. Zhang, *Microchimica Acta*, 2010, **168**, 259-265.
- 22. S. Kaneko, T. Ito, Y. Hirabayashi, T. Ozawa, T. Okuda, Y. Motoizumi, K. Hirai, Y. Naganuma, M. Soga, M. Yoshimoto and K. Suzuki, *Talanta*, 2011, **84**, 579-582.
- 23. G. Wang, X. Lu, T. Zhai, Y. Ling, H. Wang, Y. Tong and Y. Li, *Nanoscale*, 2012, **4**, 3123-3127.
- 24. C. Li, Y. Liu, L. Li, Z. Du, S. Xu, M. Zhang, X. Yin and T. Wang, *Talanta*, 2008, **77**, 455-459.
- 25. S. Deki, H. Yanagimoto, S. Hiraoka, K. Akamatsu and K. Gotoh, *Chemistry of Materials*, 2003, **15**, 4916-4922.
- 26. Y. Wang, Q. Zhu and H. Zhang, *Chemical Communications*, 2005, 5231-5233.
- 27. M. Chigane and M. Ishikawa, *Journal of the Chemical Society, Faraday Transactions*, 1998, **94**, 3665-3670.
- 28. A. P. Grosvenor, M. C. Biesinger, R. S. C. Smart and N. S. McIntyre, *Surface Science*, 2006, **600**, 1771-1779.
- 29. G. Fischer, X. Cao, N. Cox and M. Francis, Chemical Physics, 2005, 313, 39-49.
- 30. R. Linder, K. Seefeld, A. Vavra and K. Kleinermanns, Chemical Physics Letters, 2008, 453, 1-6.
- 31. D. Xie, Q. Su, Z. Dong, J. Zhang and G. Du, *CrystEngComm*, 2013, **15**, 8314-8319.
- 32. Y. Ding, Y. Liu, J. Parisi, L. Zhang and Y. Lei, Biosensors and Bioelectronics, 2011, 28, 393-398.
- 33. W. Lu, X. Qin, A. M. Asiri, A. O. Al-Youbi and X. Sun, *Analyst*, 2013, **138**, 429-433.
- 34. K. J. Cash and H. A. Clark, *Trends Mol Med*, 2010, **16**, 584-593.
- 35. X. Li, A. Hu, J. Jiang, R. Ding, J. Liu and X. Huang, *Journal of Solid State Chemistry*, 2011, **184**, 2738-2743.
- 36. R. M. Abdel Hameed, Biosensors and Bioelectronics, 2013, 47, 248-257.

- 37. J. Yang, J. H. Yu, J. Rudi Strickler, W. J. Chang and S. Gunasekaran, *Biosens Bioelectron*, 2013, 47, 530-538.
- 38. W. Lv, F.-M. Jin, Q. Guo, Q.-H. Yang and F. Kang, Electrochim. Acta, 2012, 73, 129-135.
- 39. B. Yuan, C. Xu, D. Deng, Y. Xing, L. Liu, H. Pang and D. Zhang, *Electrochim. Acta*, 2013, 88, 708-712.
- 40. X. Pang, D. He, S. Luo and Q. Cai, Sensor Actuat B: Chem, 2009, 137, 134-138.
- 41. X. Wang, C. Hu, H. Liu, G. Du, X. He and Y. Xi, Sensor Actuat B: Chem, 2010, 144, 220-225.

Figure Captions

- Fig. 1 XRD diffraction spectrum of hollow cage-like NiO nanostructures
- **Fig. 3** XPS spectra of the hollow cage-like NiO nanostructures: (a) wide scale spectrum (b) (b) Ni 2p and (c) O 1s spectra's for compositional purity
- **Fig.2** SEM image of the hollow cage-like NiO nanostructures (a, b) broad scale images with high distribution (c, d) narrow scale images showing enhanced features of individual hollow cages.
- Fig. 4 FT-IR spectra of hollow cage-like NiO nanostructures (a) before anneling (b) after anneling of precursors material
- **Scheme .1** Schematic diagram representing growth mechanism of hollow-cage like NiO nanostructures
- **Fig. 5** Cyclic voltammograms of : (Violet) bare GCE in the presence of 0.1 mM glucose, (Black) NiO HCs-Nafion/GCE in the absense and (Blue) in the presence of 0.1 mM glucose
- **Fig. 6** CV profile of NiO HCs-Nafion/GCE at various scan rates from 0.05 to 1.0 mV/s in 0.1 M NaOH with 1.0 mM glucose with inset graph of anode and cathode current vs square root of scan rate (b) CV profile for effect of NiO deposition volume on Ip response of NiO HCs-Nafion/GCE in range from 05 to 20 μ L at 0.48 V (c) CV profile for the effect of electrolytic volume on Ip response of NiO HCs-Nafion/GCE in range from 1.0 to 10.0 ml
- **Fig. 7** CV profile for NiO HCs-Nafion/GCE (a) with successive increse in glucose concentration ranging from 0.1 to 5.0 mM (b) the corresponding linear calibration plot
- **Fig. 8** CV profiles recorded for (a) selectivity of developed sensor for electroactive interferents (b) NiO HCs-Nafion/GCE reproducibility and corresponding inset bar graph showing variation of IP responces for 15 similarly prepared electrodes (c) Ip response recorded for NiO HCs-Nafion/GCE from 1 week up to 02 months of same electrode stored in ambient air conditions

Table 1 Comparison of different NiO based non enzymatic glucose sensors in terms of detection limit, linear range and sensitivity.

Type of Electrode	Performance		Sensitivity (μA mM ⁻¹ cm ⁻²)	Reference
	LOD (µM)	Linear Range (mM)	_	
NiAl-LDH	3600	0.08–2	339.2	36
CS-RGO-NiNPs	4100	up to 9	318.4	37
DNA dispersed Graphene-NiO	2.5	0.001 to 8.0	9.0	38
NiO NPs/GO/GC	1.0	0.003-3.05	1087	39
TiO ₂ /CNT/Pt/GOx	5.7	0.006–1.5	0.24	40
CuO nanorods/G	4.0	4 0-8.0	371.43	41
NiO HCs-Nafion/GCE	0.1	0.1 to 5.0 mM	2476.4	This study

Table 2 Determination of glucose level in real blood serum samples.

Samples	Concentration (mM) ⁿ		Relative standard	Glucometer
	Fasting Sugar	Random Sugar	deviation (%)	(mM)
Sample 1	4.59		0.4	4.51
Sample 2	4.61		0.1	4.65
Sample 3	4.62		0.3	4.69
Sample 4		4.7	0.1	4.5
Sample 5		5.41	0.2	5.45
Sample 6		5.49	0.1	4.52

Conditions NiO HCs-Nafion/GCE, 09 ml 0.1M NaOH, $10~\mu l$ filtered real sample (2 times diluted), no. of replications =3

Fig. 1

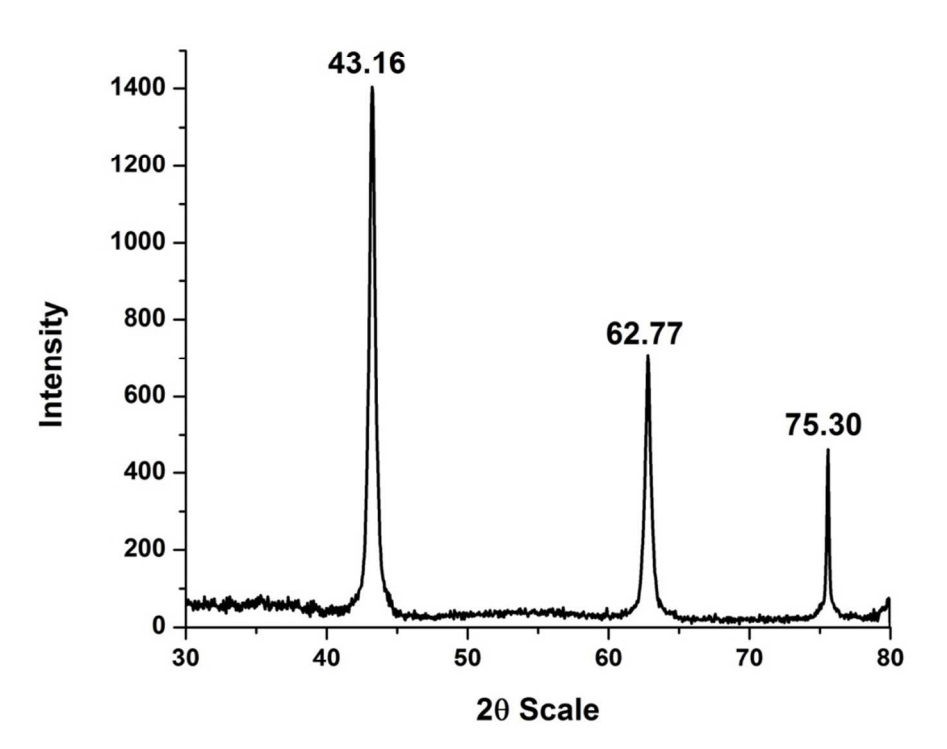


Fig. 2

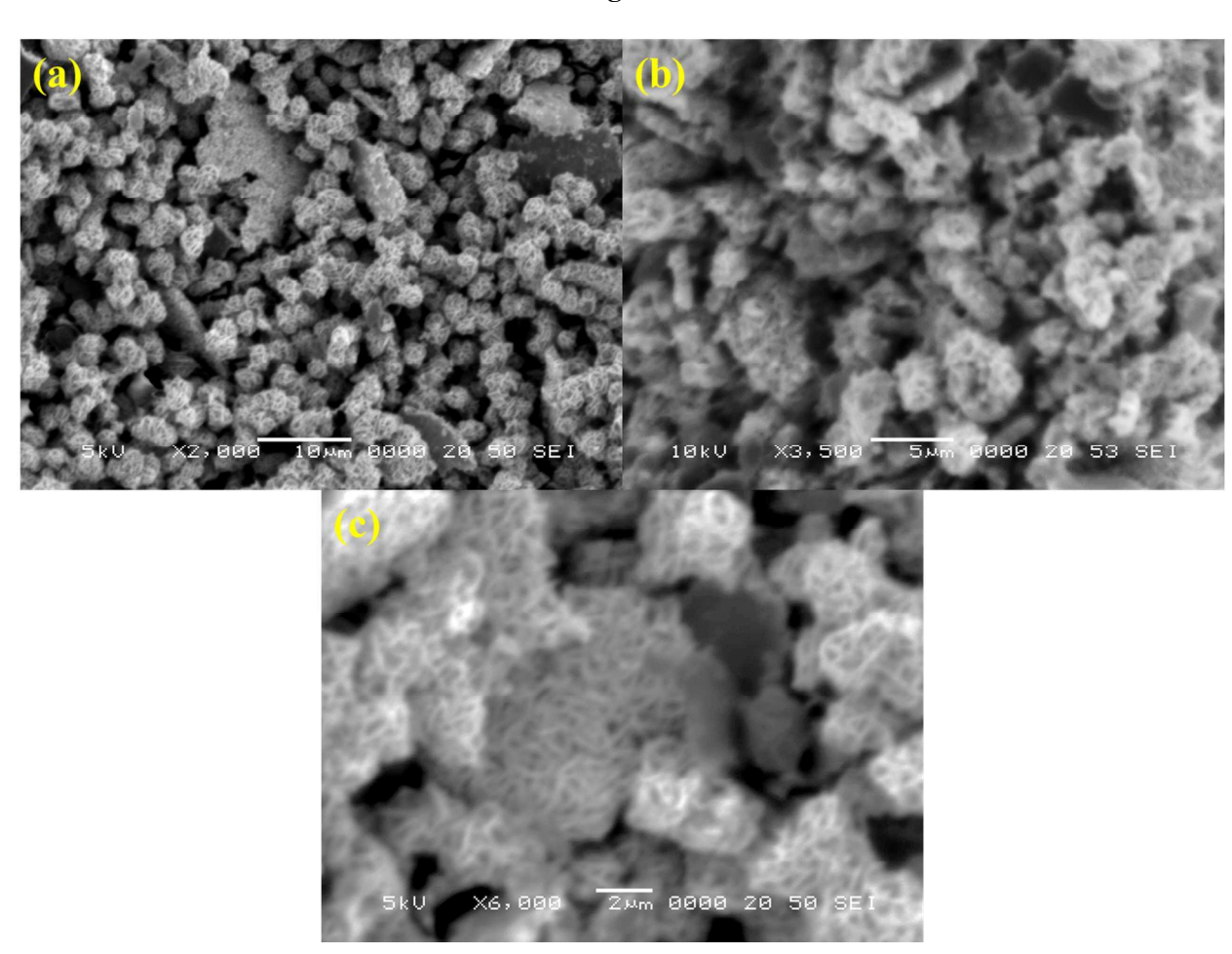


Fig. 3

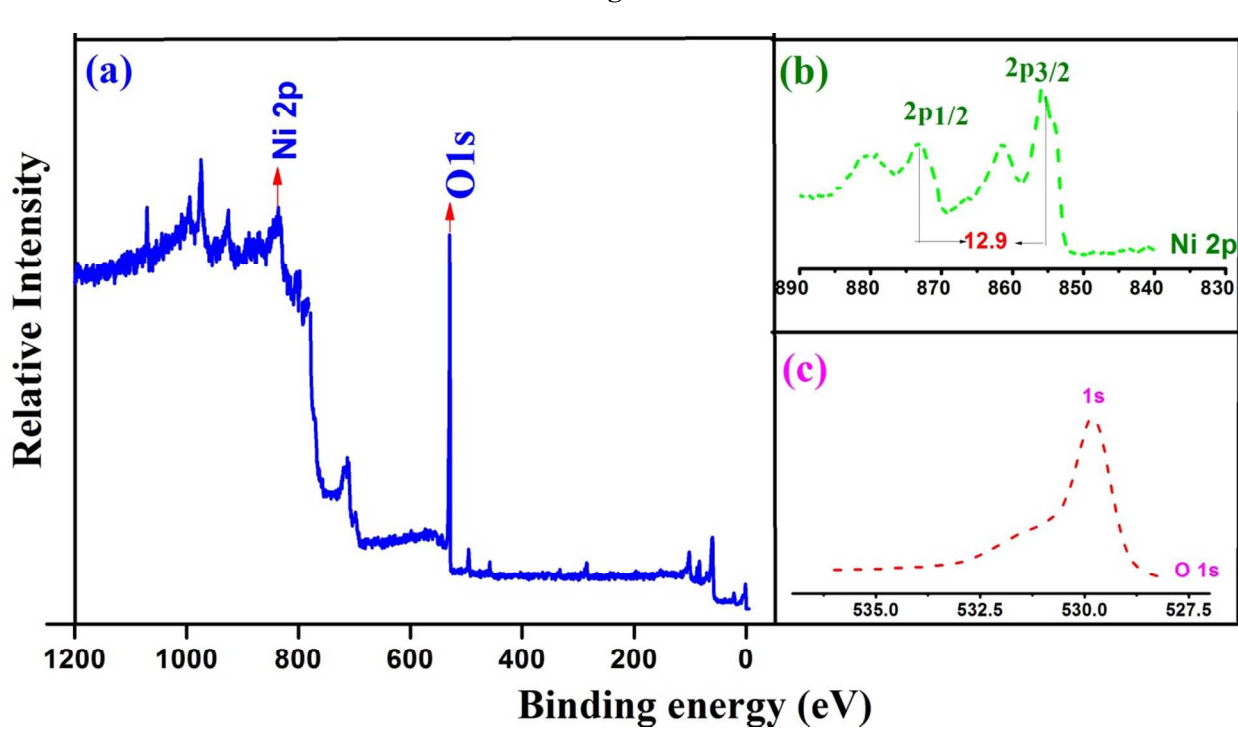
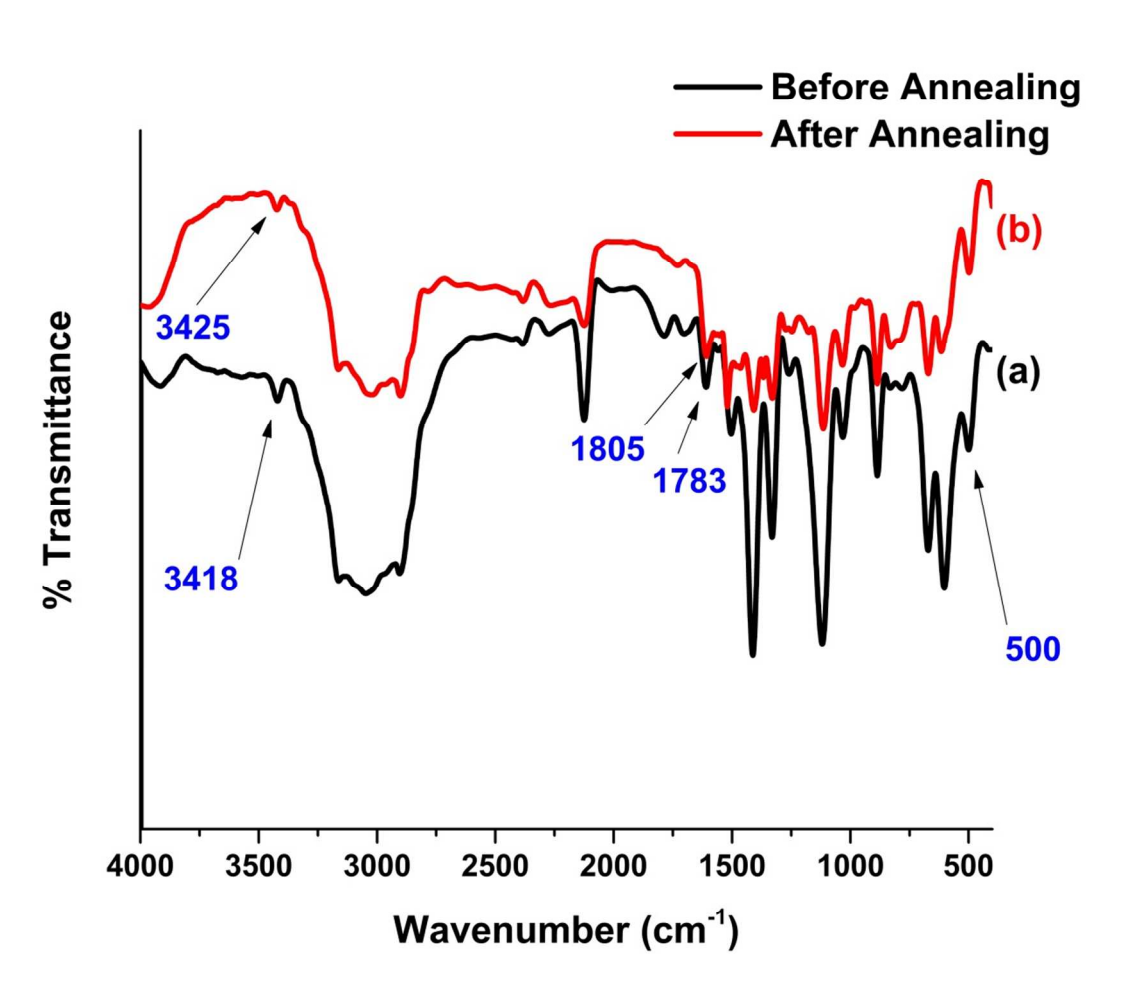


Fig. 4



Scheme. 1

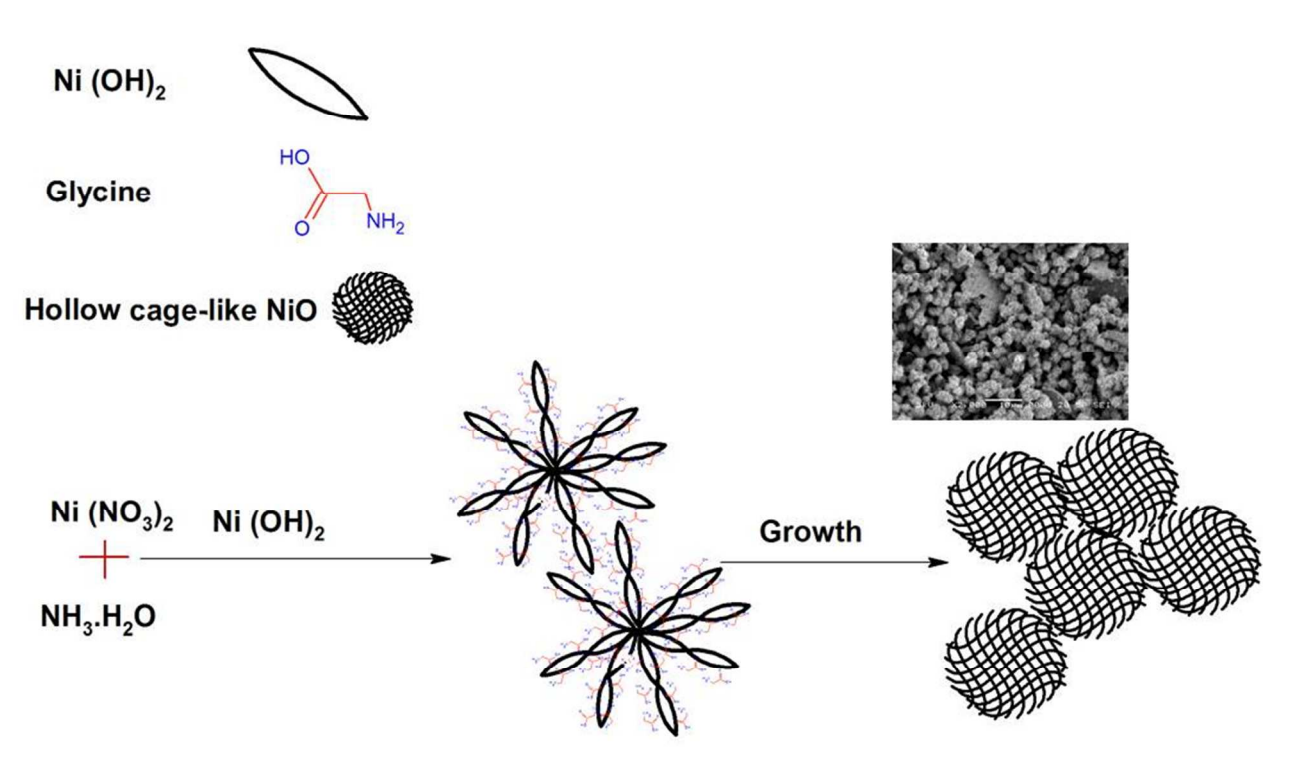


Fig. 5

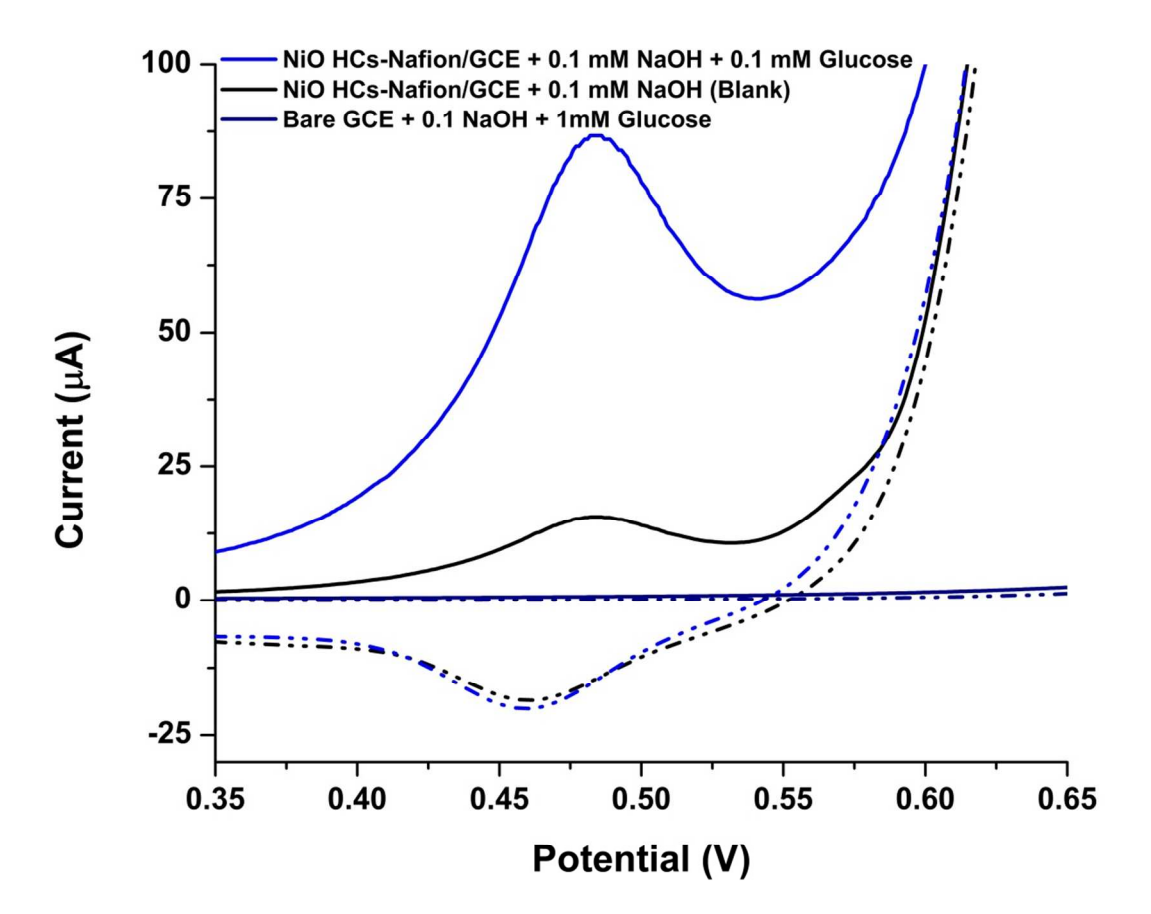


Fig. 6

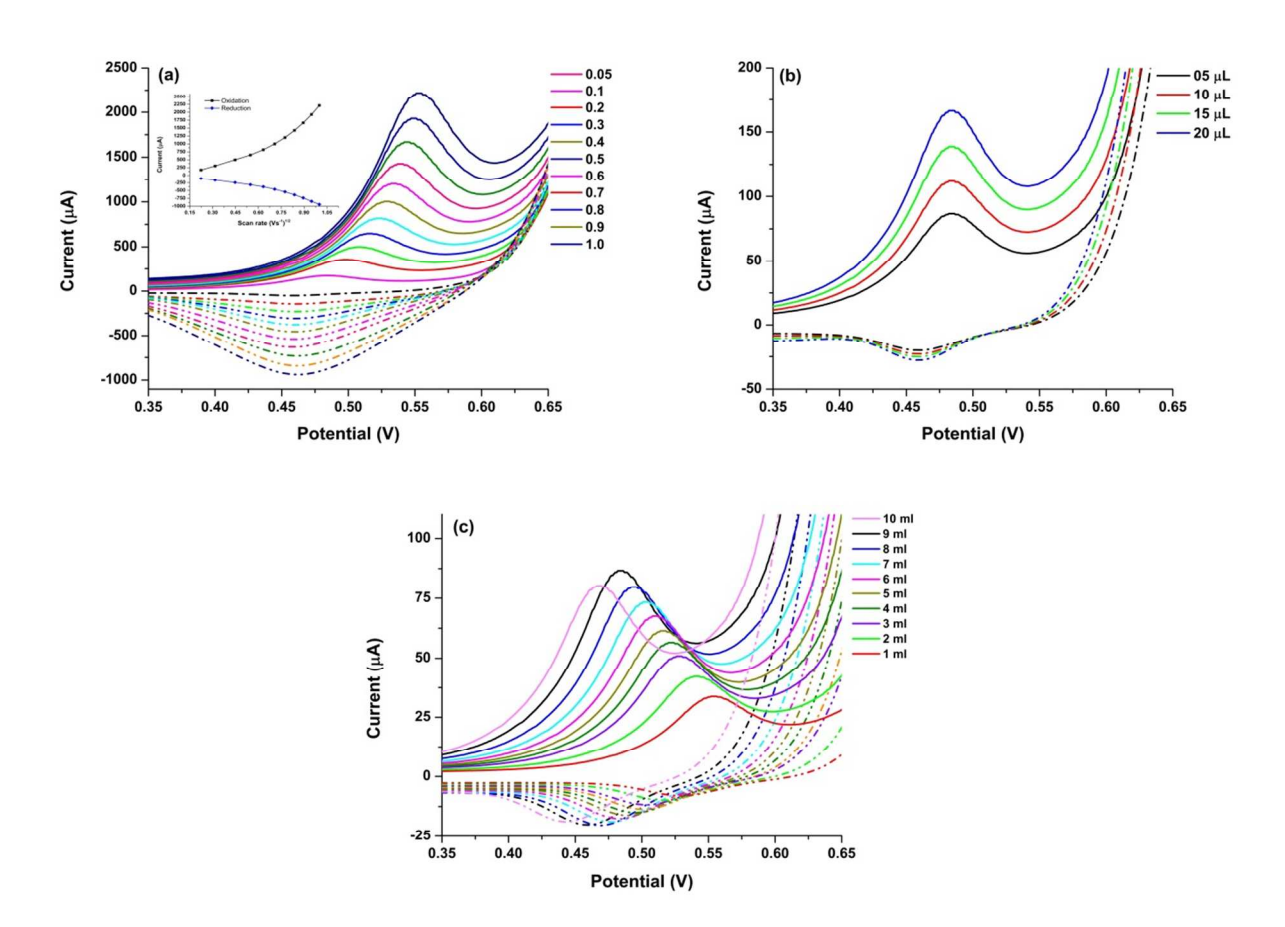


Fig. 7

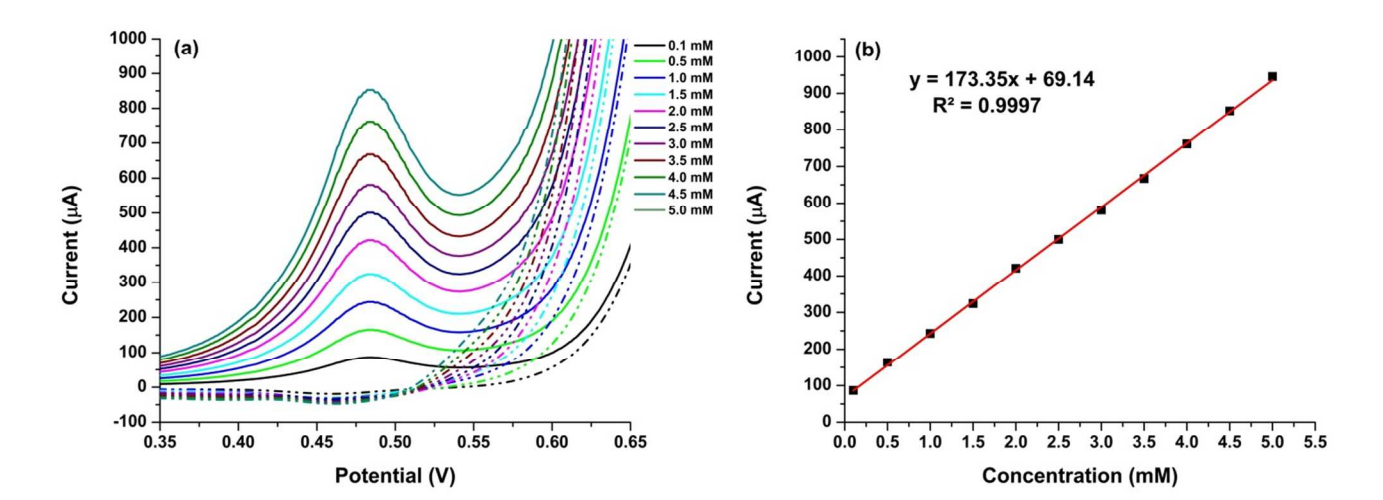
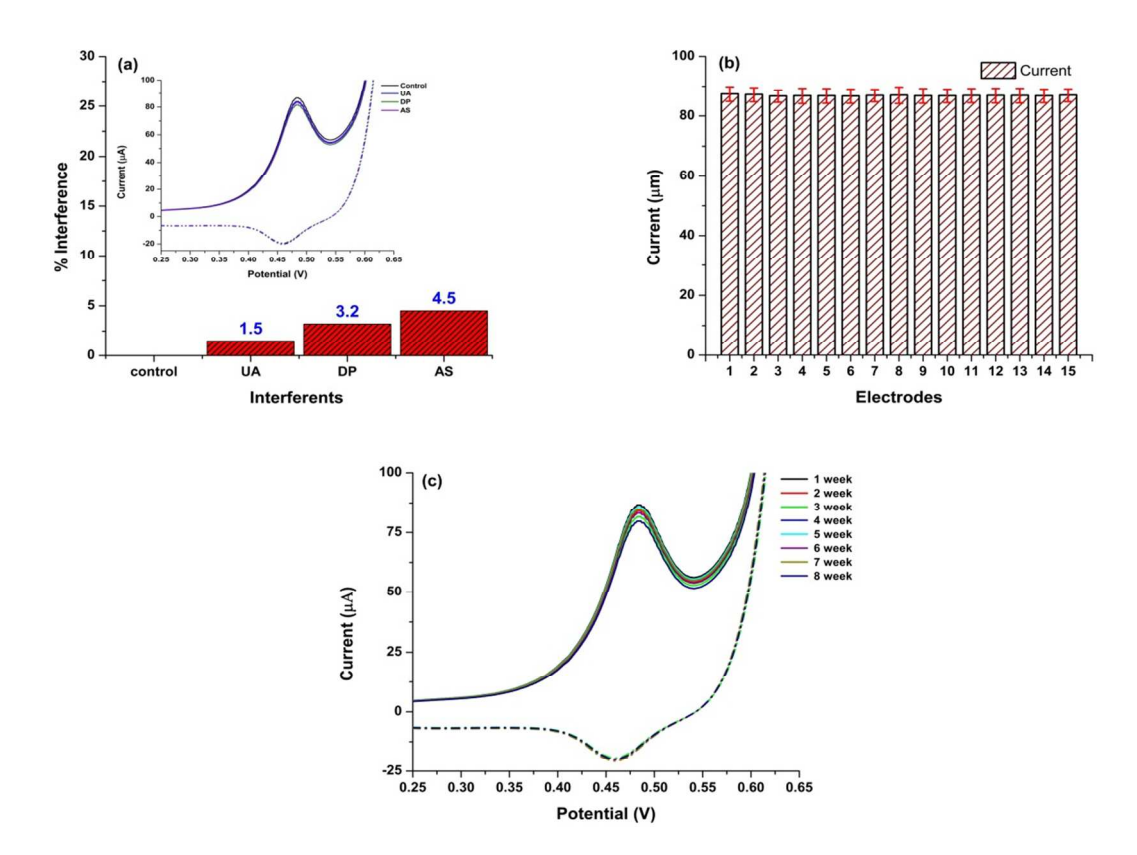


Fig. 8



Graphical Abstract

